

PREPARATION OF THIOL-FUNCTIONALIZED CELLULOSE AND ITS APPLICATION TO THE REMOVAL OF Hg(II) FROM WATER ENVIRONMENT

ZHI ZHANG,* YINGLAN CAO,* LINA CHEN* and ZHIYONG HUANG*,**

*College of Food and Biological Engineering, Jimei University, Xiamen, 361021, China

**Fujian Collaborative Innovation Center for Exploitation and Utilization of Marine Biological Resources, Xiamen, 361102, China

✉ Corresponding author: Zhiyong Huang, zhyhuang@jmu.edu.cn

Received May 4, 2015

A bio-adsorbent of thiol-functionalized cellulose (TFC) was chemically prepared for the removal of Hg(II) from aqueous solutions. The surface morphology and thiol content of TFC were characterized and measured, and the adsorption kinetics and adsorption isotherm of Hg(II) were investigated. Results showed that the maximum adsorption efficiency (99%) of the as-prepared TFC was obviously higher than that of the raw cellulose (66%). More than 96% of Hg(II) at the concentration of 1.0 mg L⁻¹ could be removed from real wastewater samples within 20 min. The adsorption behavior could be fitted by Langmuir and Freundlich models with $R^2 > 0.96$. The results demonstrated that the as-prepared TFC is a novel bio-adsorbent for the removal of Hg(II) from water environment with the advantages of rapidity, high efficiency, simple preparation and environment protection.

Keywords: bio-adsorbent, thiol-functionalized cellulose, Hg(II), water treatment

INTRODUCTION

Mercury (Hg) is one of the most toxic heavy metals because of its severely mutagenic, teratogenic and carcinogenic effects on organisms.¹ In ecosystems, Hg mainly derives from releasing sources, such as discharged urban sewage, agricultural materials, mining, fossil fuel combustion and industrial discharges, which trigger serious mercurial pollution of the water environment.² Through biochemical processes, the species of inorganic Hg in the environment are readily converted into highly toxic organic mercury, such as monomethylmercury and dimethylmercury. These organic mercury species will be assimilated and accumulated rapidly by algae, fish and shellfish.^{3,4} Considering the effects of bioaccumulation and biomagnification, even low concentrations of Hg(II) in the water environment could cause serious risks for human health through the food chain. Therefore, it is essential to develop an effective and convenient method to remove Hg(II) from the water environment.

Many technologies, such as chemical precipitation, coagulation, ion exchange, membrane filtration and physical adsorption, have been developed to remove Hg(II) from aqueous media.⁵ With the advantages of simple operation, environmental benefits and abundance of raw materials, activated carbon is extensively used as an adsorbent for Hg(II) in water treatments. However, the drawback of its high cost has seriously restricted its large-scale applications in wastewater treatment.⁶⁻⁸ Hence, much attention has been paid to the exploration of low cost and highly efficient bio-adsorbents. With abundant functional groups and high affinity to Hg(II), many natural raw materials, such as chitosan,⁹ rice husk,¹⁰ rice straw,¹¹ wheat bran,¹² and microbial biomass,¹³ have been directly used as bio-adsorbents. However, these natural raw adsorbents cannot be applied for the treatment of real samples because of their low adsorption efficiency and poor specificity.¹⁴ Therefore, efforts have been focused on the modification of the raw materials to improve the adsorption efficiency and specificity. For example, Gupta *et al.*¹⁵ prepared a thiol-functionalized sugarcane bagasse (SCB) with an adsorption capacity of 192.31 mg g⁻¹, higher than that of the virgin SCB (44.36), and the thiol-SCB was successfully applied for the removal of Hg(0) vapor from broken compact fluorescent light bulbs and Hg(II) from contaminated water streams. Wang *et al.*¹⁶ synthesized a thiourea-modified chitosan

for Hg(II) removal from wastewater with an adsorption capacity higher than that of the raw chitosan. A chelating resin containing abundant sulfamine groups has been prepared with a maximum adsorption capacity of Hg(II) more than 200 mg g⁻¹.¹⁷ Chemical modification provided the natural materials with more binding sites or additional functional groups to improve the adsorption capacities of Hg(II) in aqueous solutions.^{18,19} Sulfur-containing materials have also attracted much attention due to their high affinity to Hg. For example, thiol-incorporated and sulphurised activated carbons,^{20,21} thiol-functionalized Zn-doped biomagnetite particles,²² mercapto-grafted rice straw¹¹ and L-cysteine-functionalized mesoporous silica²³ have been synthesized and successfully applied to the removal of Hg(II) from aqueous solutions.

Plant cellulose, an abundant natural biopolymer, with the formula of (C₆H₁₀O₅)_n, is a category of polysaccharides consisting of linear chains with hundreds to over ten thousand β-(1,4) linked D-glucose units. With a large quantity of hydroxyl groups and flexible polymer chain, cellulose has been widely used as a bio-adsorbent to remove heavy metals from aqueous solutions.^{24,25} However, natural raw cellulose presents low adsorption capacities for heavy metals, especially for Hg(II).²⁶ For the purpose of increasing the adsorption efficiency, partial or full surface modification was required.²⁷ Thiol-functionalization is one of the most important methods for cellulose modification. For example, thiosemicarbazide with C=S and amino groups has been grafted onto the surface of cellulose for heavy metal removal from aqueous solutions.²⁷ Cellulose modified with mercaptobenzothiazole exhibited high adsorption efficiencies to Hg(II) in aqueous solutions due to soft-soft interaction.²⁸ Although many thiol-functionalized celluloses have been prepared, there are few studies about the thiol-functionalized cellulose synthesized using mercaptoacetic acid as thiol reagent, and its application for the rapid removal of Hg(II).

In the present study, a bio-adsorbent of thiol-functionalized cellulose (TFC) was prepared using mercaptoacetic acid as thiol reagent, and the morphology of TFC was characterized. The adsorption behaviors of TFC to Hg(II) in aqueous solutions were evaluated and discussed.

EXPERIMENTAL

Materials

Cellulose was purchased from Henan Huikang Industrial General Co., Ltd, China. Mercury chloride was obtained from Guizhou Tongren Yinhu Chemical Co., Ltd, China. Mercaptoacetic acid and acetic anhydride were supplied by Sinopharm Chemical Reagent Co., Ltd, China. 5,5'-dithiobis (2-nitrobenzoic acid) was purchased from Sigma Aldrich, USA. The other chemicals, such as sodium hydroxide, acetic acid, sulphuric acid, and thiourea, were obtained from Xilong Chemical Co., Ltd, China. All reagents were of analytical grade. Deionized water (18.2 MΩ·cm) (TKA Genpure series, Germany) was used throughout the experiment.

Preparation of thiol-functionalized cellulose

The thiol-functionalized cellulose was prepared based on the methods proposed by Celo *et al.*²⁹ and Lee and Mowrer³⁰ with some modification. Briefly, 100 mL of mercaptoacetic acid, 60 mL of acetic anhydride, 40 mL of acetic acid, and 0.3 mL of concentrated sulphuric acid were mixed in a flask and stirred thoroughly. After cooling to room temperature, 30 g of cellulose was impregnated in the mixed solution. The reaction was maintained at 40 °C for 3 days to yield the thiol-functionalized cellulose (TFC). The TFC was collected by vacuum filtration, and washed with water. After drying at 40 °C under vacuum, the TFC was stored in a brown container at 4 °C. The thiol-functionalization reaction is shown in Figure 1.

Characterization of TFC

TFC coated with a thin layer of platinum was characterized by scanning electron microscopy (SEM) (Hitachi, Japan) at accelerating voltage from 10 to 15 kV. Infrared spectroscopic analysis was performed on a Nicolet 380 Fourier transform infrared spectrometer (Thermo scientific, US) with KBr pellets at a mass ratio of 100:1.

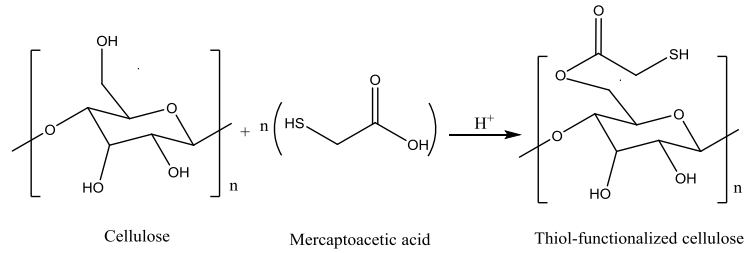


Figure 1: Schematic reaction of cellulose and mercaptoacetic acid

Determination of thiol groups

The amounts of thiol groups (-SH) were measured with Ellman's method³¹ with some modification. Briefly, 0.2 g of TFC was hydrated with 2 mL of deionized water, then 2 mL of 0.5 mol L⁻¹ phosphate buffer (pH 8.0) and 4 mL of Ellman's reagent (3 mg of 5, 5'-dithiobis (2-nitrobenzoic acid) in 10 mL of 0.5 mol L⁻¹ phosphate buffer, pH 8.0) were sequentially added. After incubation for 3 h at room temperature, the hydrated TFC was centrifuged (3260×g) for 10 min, and the supernatant was spectrophotometrically measured at 412 nm with an ultraviolet-visible spectrophotometer (UV-2100, LabTech Holdings, Inc. Beijing). Mercaptoacetic acid was used as a standard to calibrate the measurement.

Measurement of Hg concentrations

The concentrations of Hg in all the solutions were measured with a hydride generation atomic fluorescence spectrometry (HG-AFS) (AFS-640, Beijing Ruili Instrumental Co., China). The accuracy and precision of the measurement were evaluated using three levels of standard additions with an average recovery of 101%. The detection limit was calculated to be 0.026 µg L⁻¹ with 3 times the standard deviations (n=8).

Adsorption

Adsorption experiments were performed by adding 50 mg of TFC in Hg(II) solutions (50 mL) with various concentrations. After oscillation at 25 °C for a certain time, the supernatants were collected by syringe filters (0.45 µm). All of the experiments were carried out in triplicates. Hg(II) concentrations in all the supernatants were measured with HG-AFS as described above.

Hg(II) solutions (1 mg L⁻¹) at different pH values from 2.0 to 9.0 adjusted by 0.1 mol L⁻¹ NaOH and 0.1 mol L⁻¹ HCl were used for pH optimization. After adsorption for 120 min, the concentrations of Hg(II) in suspensions were measured, and the adsorption efficiencies (%) were calculated by the following formula:

$$\text{Adsorption efficiency (\%)} = \frac{C_0 - C_e}{C_0} \times 100 \quad (1)$$

where C_0 is the initial Hg(II) concentration (mg L⁻¹), C_e is the equilibrium Hg(II) concentration (mg L⁻¹) after adsorption.

Hg(II) mixed with 50 mg TFC at pH 4.0 was used for the test of adsorption kinetics.

Hg(II) with different initial concentrations from 0.5 to 25 mg L⁻¹ at pH 4.0 was used for the study of the adsorption isotherm. The adsorption capacity (q_e , mg g⁻¹) was calculated by the formula:

$$q_e = \frac{(C_0 - C_e) \times v}{m} \quad (2)$$

where C_0 and C_e are the initial and equilibrium concentrations of Hg(II) (mg L⁻¹), respectively; V is the solution volume (L) and m is the mass of TFC (g).

Desorption

Based on the methods of Hakami *et al.*³² and Shade,³³ 30 mL of 3 mol L⁻¹ HCl or 3 mol L⁻¹ HCl containing 2% (m/v) thiourea was respectively used for desorption. After oscillation for 30 min, the suspensions were separated using a syringe filter (0.45 µm). The desorption efficiency (%) was calculated by the amount of Hg(II) in the solutions *versus* the total amount of Hg(II) loaded in TFC.

Adsorption of Hg in effluents

Wastewater was collected from a local sewage treatment plant for treating a real sample. Since the concentration of Hg(II) in the wastewater was below $1.0 \mu\text{g L}^{-1}$ based on our measurement, artificial Hg(II) at two levels was added for TFC adsorption. After adjusting the pH at 4.0, the effluent samples were added with 50 mg of TFC. The mixture was oscillated for 20 min. The adsorption efficiencies (%) were calculated.

RESULTS AND DISCUSSION

Characteristics of TFC

The SEM images of raw cellulose, TFC, TFC after adsorption and TFC after desorption are shown in Figure 2. The raw cellulose presents a smooth surface with a great number of tiny stripes, and the TFC shows a rough and uneven surface, indicating successful thiol-modification on the surface of cellulose. The phenomenon of granular adhesion is observed on the surface of TFC after adsorption, which possibly derived from the interactions of Hg(II) and -SH. The surfaces of TFC became smooth and homogeneous after desorption, suggesting broken bonds of Hg(II) and -SH. The FTIR spectrum of raw cellulose in Figure 3a shows that the peak at 3349 cm^{-1} derived from the O-H stretching vibration in cellulose. Two strong bands at 2875 cm^{-1} and $1300\text{-}1500 \text{ cm}^{-1}$ were assigned to C-H stretching vibration of methyl and methylene radicals, which are the characteristic features of cellulose, hemicelluloses and lignin.¹¹ The peak at 1799 cm^{-1} was assigned to the carbonyl group.²⁸ The weak band at 1548 cm^{-1} was attributed to the C=C stretching vibration of aromatic or alkene groups in cellulose. The peaks at 873 cm^{-1} could be assigned to the C-O-C carbohydrate stretching group. Moreover, the peaks at 1112 cm^{-1} and 1033 cm^{-1} were attributed to the ring stretching of glucose and C-O stretching vibration in cellulose, respectively.²⁸ The spectrum of TFC (Fig. 3b) is similar to that of the raw cellulose. An additional weak characteristic peak at 2563 cm^{-1} was assigned to S-H stretching vibration,^{32,34,35} suggesting that the cellulose has been functionalized with -SH. The peaks of TFC after adsorption at 2563 cm^{-1} , 1731 cm^{-1} , 1469 cm^{-1} and 1456 cm^{-1} (Fig. 3c) disappeared and the O-H band shifted from 3346 cm^{-1} to 3353 cm^{-1} , indicating the interaction of TFC with Hg(II).²⁸

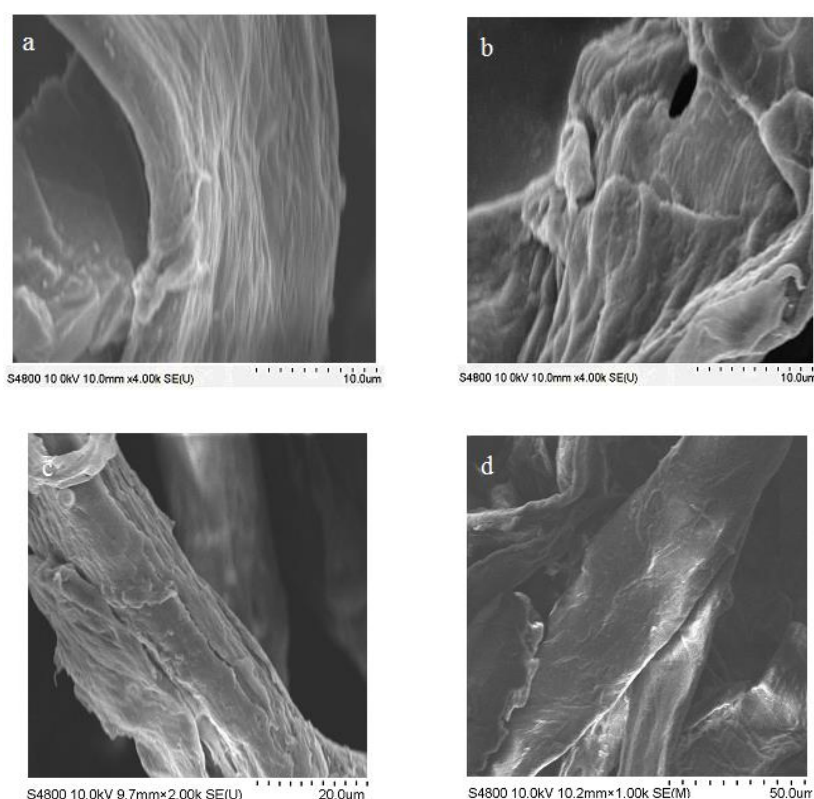


Figure 2: SEM images of raw cellulose (a), thiol-functionalized cellulose (TFC) (b), TFC after adsorption (c), and TFC after desorption (d)

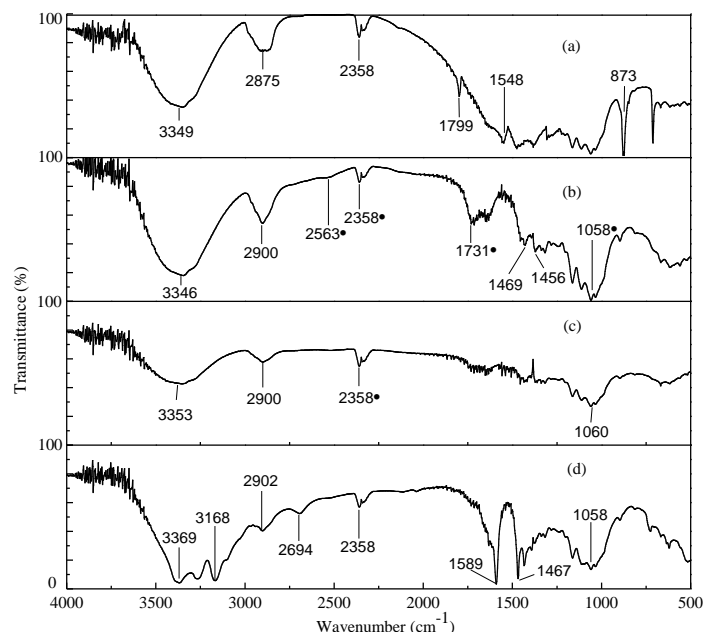


Figure 3: FTIR spectra of raw cellulose (a), thiol-functionalized cellulose (TFC) (b), TFC after adsorption (c), and TFC after desorption (d)

Based on our measurement, the amount of thiol groups grafted on TFC was $39.7 \pm 2.9 \mu\text{mol g}^{-1}$. The adsorption efficiency for 1 mg L^{-1} of Hg(II) was 99%, much higher than that (66%) of the raw cellulose. The result suggested that the features of TFC, such as surface area, pore structure and functional groups, have been significantly improved after thiol-functionalization.^{11,28,36} Similar results were also found in previous reports. For example, Song *et al.*¹¹ found that the mercapto-grafted rice straw presented a strong affinity to Hg(II) with a maximum adsorption capacity of 161.3 mg g^{-1} in water solution, which was superior to that of the raw rice straw (103.1 mg g^{-1}). Gupta *et al.*¹⁵ observed that the adsorption capacity of thiol-functionalized sugarcane bagasse was 4.3 times higher than that of the virgin sugarcane bagasse.

Effect of pH on adsorption

The pH value is a critical factor affecting the surface properties of adsorbents and the speciation forms of metal ions in aqueous solutions.³⁷ However, the pH values ranging from 2.0 to 4.0 showed no obvious influence on the Hg(II) adsorption, as illustrated in Figure 4. However, the adsorption efficiencies slightly decreased at pH values above 4.0, which might be derived from the formation of HgOH^+ and Hg(OH)_2 species.^{28,38} Considering economic interests and operation convenience, a pH value of 4.0 was selected as the optimum.

Adsorption kinetics

Adsorption kinetics (Fig. 5) shows that the adsorption efficiencies of TFC rapidly increased in the first 5 min, in which about 70% of Hg(II) was adsorbed. Then, the adsorption rates decreased and the adsorption equilibrium was reached in 20 min. At the initial stage, the rapid adsorption might be attributed to the presence of a large quantity of binding sites on the TFC surfaces. However, the occupation of binding sites resulted in a low adsorption rate in the latter stage.^{28,32} In the present study, 20 min of the adsorption equilibrium time was less than those reported previously for Hg(II) adsorption. For example, the equilibrium time of thiol-functionalized biomass was up to 90 min.³⁴ The adsorption equilibrium of *Ulva lactuca*³⁹ and chemically modified rice straw¹¹ was up to 2 h.

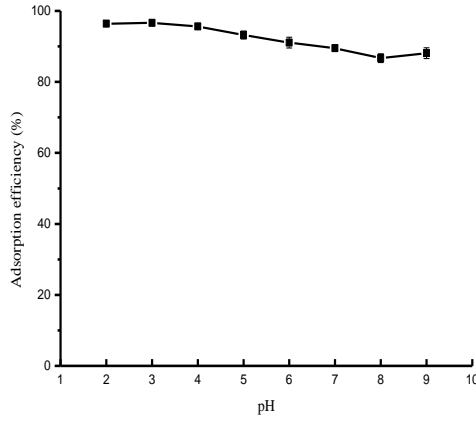


Figure 4: Effect of pH on Hg(II) adsorption by TFC

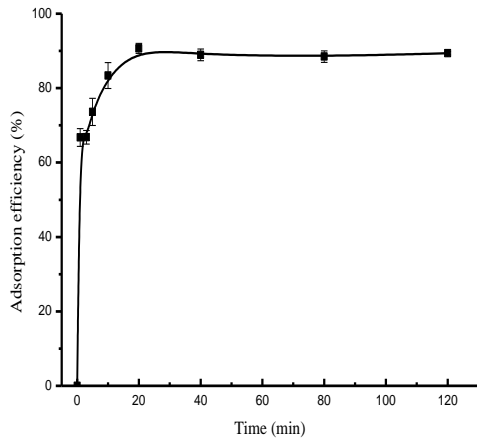


Figure 5: Adsorption efficiency versus adsorption time

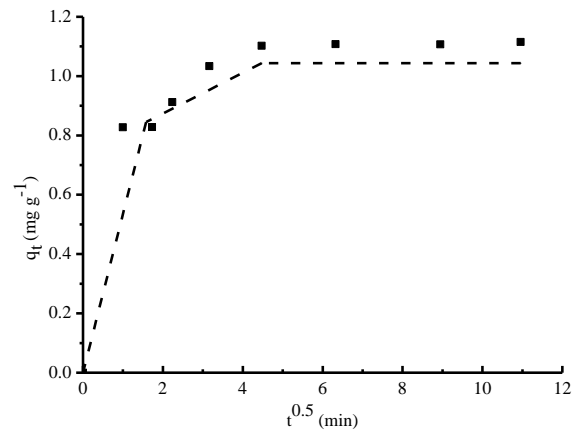


Figure 6: Fitting curve of Weber-Morris model for the adsorption of Hg(II) by TFC

The pseudo-first-order model, pseudo-second-order model and Weber-Morris diffusion kinetic model were used to fit the adsorption kinetics data:

$$\text{Pseudo-first-order:}^{40} \quad \log(q_e - q_t) = \log q_e - \frac{k_1}{2.303} t \quad (3)$$

$$\text{Pseudo-second-order:}^{40} \quad \frac{t}{q_t} = \frac{1}{k_2 q_e^2} + \frac{t}{q_e} \quad (4)$$

$$\text{Weber and Morris:}^{41} \quad q_t = k_{id} t^{0.5} + c \quad (5)$$

where q_e (mg g⁻¹) and q_t (mg g⁻¹) are the amounts of Hg(II) adsorbed onto the TFC at equilibrium and at a certain time of t (min), respectively; k_1 (min⁻¹), k_2 (g mg⁻¹ min⁻¹) and k_{id} (mg g⁻¹ min^{-0.5}) are the rate constants; c is the intercept (mg g⁻¹).

The data in Table 1 show that the pseudo-second-order model fitted the experimental data with a correlation coefficient of $R^2 > 0.999$. The calculated q_e (1.122 mg g⁻¹) was in good agreement with the measured value (1.115 mg g⁻¹). The fitting curve of the Weber-Morris model in Figure 6 indicates that the adsorption was not solely determined by the rate-control process, because the fitting curve does not pass through zero with an intercept of 0.8628 mg g⁻¹. Three stages, including external mass transfer, intraparticle diffusion and saturation, were used to describe the adsorption process. The rapid adsorption in the first stage was attributed to the external surface adsorption, and the equilibrium stage was assigned to the intraparticle diffusion of Hg in TFC.⁴²

Table 1
Parameters of adsorption kinetic models at 25 °C

| Experimental value q_e (mg g ⁻¹) | Pseudo-first-order | | | Pseudo-second-order | | | Weber and Morris | | |
|---|----------------------------|-----------------------------|--------|---|-----------------------------|--------|--|---------------------------|--------|
| | k_1 (min ⁻¹) | q_e (mg g ⁻¹) | R^2 | k_2 (g mg ⁻¹ min ⁻¹) | q_e (mg g ⁻¹) | R^2 | k_{id} (mg g ⁻¹ min ^{-0.5}) | C (mg g ⁻¹) | R^2 |
| 1.115 | 0.1108 | 0.1572 | 0.6741 | 1.191 | 1.122 | 0.9999 | 0.0291 | 0.8628 | 0.6680 |

Table 2
Parameters of isotherm models for Hg(II) adsorption by TFC

| Adsorbent | Langmuir isotherm model | | | Freundlich isotherm model | | |
|-----------|-----------------------------|---------------------------|--------|--|--------|--------|
| | q_m (mg g ⁻¹) | b (L mg ⁻¹) | R^2 | K_f ((mg g ⁻¹)(L mg ⁻¹) ^{1/n}) | $1/n$ | R^2 |
| TFC | 11.00 | 0.9670 | 0.9631 | 3.931 | 0.4183 | 0.9622 |

Table 3
Characteristics of the effluent collected from Jimei Sewage Treatment Plant, China

| pH | COD (mg L ⁻¹) | Concentration of metal ions (µg L ⁻¹) | | | | | | | |
|------|------------------------------|---|-----|------|------|------|--------|-------|-------|
| | | Cr | Mn | Ni | Cu | Zn | Cd | Pb | Hg |
| 6.20 | 3.37 | 5.40 | 417 | 20.4 | 22.9 | 17.4 | 0.0390 | 0.311 | 0.090 |

Table 4
Removal of Hg(II) from real effluents

| Two levels of Hg(II) | Hg concentrations (mg L ⁻¹) | | Removal efficiency (%) |
|----------------------|---|------------------|------------------------|
| | Before adsorption | After adsorption | |
| 1 | 1 | 0.033±0.004 | 96.7 |
| 2 | 10 | 1.81±0.24 | 81.9 |

The phenomenon of multilinear adsorption revealed that the adsorption has two simultaneous mechanisms: surface adsorption and intraparticle diffusion. Similar results have been also observed in previous reports. For example, Song *et al.*¹¹ found that the adsorption of Hg(II) by rice straw and mercapto-grafted rice straw followed the multilinear adsorption mechanisms; and the biosorption of Cu(II), Cd(II) and Pb(II) by *Phormidium* sp.-dominated mat biomass also followed the multilinear adsorption stages.⁴³

Adsorption isotherms

Langmuir⁴⁴ and Freundlich models⁴⁵ in formula (4) and (5) were respectively used to fit the data of the adsorption isotherms.

$$\text{Langmuir: } \frac{c_e}{q_e} = \frac{c_e}{q_m} + \frac{1}{q_m b} \quad (6)$$

$$\text{Freundlich: } \ln q_e = \frac{1}{n} \ln c_e + \ln K_f \quad (7)$$

where C_e (mg L^{-1}) is the equilibrium concentration of Hg(II) in solution, q_e (mg g^{-1}) is the amount of Hg(II) adsorbed on the TFC at equilibrium, q_m (mg g^{-1}) is the maximum adsorption capacity, b (L mg^{-1}) is the Langmuir constant related to the affinity of binding sites and the adsorption energy, K_f (mg g^{-1}) (L mg^{-1})^{1/n} is the Freundlich constant related to the adsorption capacity, and n is the heterogeneity factor.

The parameters in Table 2 illustrate that the two models were able to fit the experimental data ($R^2 > 0.96$). The maximum adsorption capacity (q_m) by the Langmuir model was 11.0 mg g^{-1} . The Freundlich parameter of the heterogeneity factor (n) gave the value of 2.39, indicating a strong interaction between TFC and Hg(II).⁴⁶ Although the q_m value was lower than the data reported in some other studies,^{16,17} it was much higher than those of 2-mercaptobenzothiazole clay (2.71 mg g^{-1}) and guava (*Psidium guajava*) bark (3.36 mg g^{-1}).^{47,48}

Desorption

The desorption of TFC-Hg was performed using hydrochloric acid through the exchange of Hg(II) and H^+ .^{11,49} The results showed that a desorption reagent of HCl (3 mol L^{-1}) containing 2% (w/v) of thiourea could effectively desorb Hg(II) with a desorption efficiency of 94%. The high desorption efficiency might be due to the formation of a soluble Hg-thiourea complex.^{32,33} The thiol binding sites were then protonated in acid media.

Treatment of real effluents

A real effluent sample collected from a local sewage treatment plant was measured to give some physical and chemical indexes, as listed in Table 3. Two levels of the Hg(II) standard solution were investigated to verify the practicality of TFC. The results in Table 4 show that the removal efficiencies of Hg(II) were of 97% and 82% at Hg concentrations of 1 mg L^{-1} and 10 mg L^{-1} , respectively. The lower removal efficiency at high concentration might be due to the insufficient quantity of TFC because the adsorption capacity of TFC was 8.2 mg g^{-1} , which was close to the maximum adsorption capacity (q_m) obtained by the Langmuir model, as described above. The results confirmed that the TFC could be used to effectively remove Hg(II) from real effluents, especially at low levels of Hg concentration.

CONCLUSION

Thiol-functionalized cellulose was chemically prepared and characterized for the adsorption of Hg(II) from aqueous solutions. The optimized pH for the adsorption was 4.0, and the adsorption equilibrium time was less than 20 min. The adsorption kinetics followed the pseudo-second-order model, and the adsorption isotherm complied with the Langmuir and Freundlich models. With a high adsorption efficiency, the TFC could be used to rapidly and effectively remove the Hg(II) present in low concentrations in wastewater.

ACKNOWLEDGEMENT: The work was supported by grants from Fujian Provincial Key Laboratory

of Food Microbiology and Enzyme Engineering (M20140902); the Foundation of the Key Project Laboratory of Urban Environment and Health, Institute of Urban Environment, Chinese Academy of Sciences (KLUEH201303), and the Foundation for Innovative Research Team of Jimei University (2010A007).

REFERENCES

- ¹ L. Järup, *Br. Med. Bull.*, **68**, 167 (2003).
- ² P. Miretzky and A. F. Cirelli, *J. Hazard. Mater.*, **167**, 10 (2009).
- ³ T. W. Clarkson, *J. Trace Elem. Exp. Med.*, **11**, 303 (1998).
- ⁴ E. J. Kerin, C. C. Gilmour, E. Roden, M. T. Suzuki, J. D. Coates *et al.*, *Appl. Environ. Microbiol.*, **72**, 7919 (2006).
- ⁵ F. L. Fu and Q. Wang, *J. Environ. Manage.*, **92**, 407 (2011).
- ⁶ P. J. Chen and M. Lin, *Water Res.*, **35**, 2385 (2001).
- ⁷ F. D. Natale, A. Erto, A. Lancia and D. Musmarra, *J. Hazard. Mater.*, **192**, 1842 (2011).
- ⁸ K. Ranganathan, *Carbon*, **41**, 1087 (2003).
- ⁹ S. Kushwaha, B. Sreedhar and P. Padmaja, *J. Chem. Eng. Data*, **55**, 4691 (2010).
- ¹⁰ M. Ahmaruzzaman and V. K. Gupta, *Ind. Eng. Chem. Res.*, **50**, 13589 (2011).
- ¹¹ S. T. Song, N. Saman, K. Johari and H. Mat, *Ind. Eng. Chem. Res.*, **52**, 13092 (2013).
- ¹² M. A. Farajzadeh and A. B. Monji, *Sep. Purif. Technol.*, **38**, 197 (2004).
- ¹³ S. K. Das, A. R. Das and A. K. Guha, *Environ. Sci. Technol.*, **41**, 8281 (2007).
- ¹⁴ D. Sud, G. Mahajan and M. P. Kaur, *Bioresour. Technol.*, **99**, 6017 (2008).
- ¹⁵ A. Gupta, S. R. Vidyarthi and N. Sankararamakrishnan, *J. Environ. Chem. Eng.*, **2**, 1378 (2014).
- ¹⁶ L. Wang, R. Xing, S. Liu, S. B. Cai, H. H. Yu *et al.*, *Int. J. Biol. Macromol.*, **46**, 524 (2010).
- ¹⁷ Y. X. Qi, X. L. Jin, C. Yu, Y. Wang, L.Q. Yang *et al.*, *Chem. Eng. J.*, **233**, 315 (2013).
- ¹⁸ T. A. H. Nguyen, H. H. Ngo, W. S. Guo, J. Zhang, S. Liang *et al.*, *Bioresour. Technol.*, **148**, 574 (2013).
- ¹⁹ W. S. Wan Ngah and M. A. K. M. Hanafiah, *Bioresour. Technol.*, **99**, 3935 (2008).
- ²⁰ F. Kazemi, H. Younesi, A. A. Ghoreyshi, N. Bahramifar and A. Heidari, *Process Saf. Environ.*, **100**, 22 (2016).
- ²¹ K. A. Krishnan and T. S. Anirudhan, *J. Hazard. Mater.*, **92**, 161 (2002).
- ²² F. He, W. Wang, J. W. Moon, J. Howe, E. M. Pierce *et al.*, *ACS Appl. Mater. Interfaces*, **4**, 4373 (2012).
- ²³ Q. Li, Z. Wang, D. M. Fang, H. Y. Qu, Y. Zhu *et al.*, *New J. Chem.*, **38**, 248 (2014).
- ²⁴ D. W. O'Connell, C. Birkinshaw and T. F. O'Dwyer, *Bioresour. Technol.*, **99**, 6709 (2008).
- ²⁵ L. Tofan, C. Paduraru, C. Teodosiu and O. Toma, *Cellulose Chem. Technol.*, **49**, 219 (2015).
- ²⁶ Y. M. Zhou, X. Y. Hu, M. Zhang, X. F. Zhou and J. Y. Niu, *Ind. Eng. Chem. Res.*, **52**, 876 (2013).
- ²⁷ S. Hokkanen, A. Bhatnagar and M. Sillanpää, *Water Res.*, **91**, 156 (2016).
- ²⁸ A. Santhana Krishna Kumar, S. Kalidhasan, V. Rajesh and N. Rajesh, *Ind. Eng. Chem. Res.*, **52**, 11838 (2013).
- ²⁹ V. Celso, R. V. Ananth, S. L. Scott and D. R. S. Lean, *Anal. Chim. Acta*, **516**, 171 (2004).
- ³⁰ Y. Lee and J. Mowrer, *Anal. Chim. Acta*, **221**, 259 (1989).
- ³¹ M. D. Hornof, C. E. Kast and A. Bernkop-Schnürch, *Eur. J. Pharm. Biopharm.*, **55**, 185 (2003).
- ³² O. Hakami, Y. Zhang and C. J. Banks, *Water Res.*, **46**, 3913 (2012).
- ³³ C. W. Shade, *Environ. Sci. Technol.*, **42**, 6604 (2008).
- ³⁴ L. Chai, Q. Wang, Q. Li, Z. Yang and Y. Wang, *Water Sci. Technol.*, **62**, 2157 (2010).
- ³⁵ J. Coates, in "Interpretation of Infrared Spectra. A Practical Approach", edited by R. A. Meyers, John Wiley & Sons, 2000, pp. 10815-10837.
- ³⁶ M. A. Martín-Lara, G. Blázquez, A. Ronda, A. Pérez and M. Calero, *Ind. Eng. Chem. Res.*, **52**, 10809 (2013).
- ³⁷ A. Gundogdu, D. Ozdes, C. Duran, V. N. Bulut, M. Soylak *et al.*, *Chem. Eng. J.*, **153**, 62 (2009).
- ³⁸ A. Santhana Krishna Kumar, S. Kalidhasan, V. Rajesh and N. Rajesh, *Ind. Eng. Chem. Res.*, **51**, 11312 (2012).
- ³⁹ Y. Zeroual, A. Moutaouakkil, F. Zohra Dzairi, M. Talbi, P. Ung Chung *et al.*, *Bioresour. Technol.*, **90**, 349 (2003).
- ⁴⁰ Y. S. Ho and G. McKay, *Process Biochem.*, **34**, 451 (1999).
- ⁴¹ W. J. Weber and J. C. Morris, *J. Sanit. Eng. Div. Am. Soc. Civ. Eng.*, **89**, 31 (1963).

- ⁴² A. E. Ofomaja, *Bioresour. Technol.*, **101**, 5868 (2010).
- ⁴³ D. Kumar and J. P. Gaur, *Bioresour. Technol.*, **102**, 633 (2011).
- ⁴⁴ I. Langmuir, *J. Am. Chem. Soc.*, **38**, 2221 (1916).
- ⁴⁵ H. M. F. Freundlich, *J. Phys. Chem.*, **57**, 292 (1906).
- ⁴⁶ G. Mckay, H. S. Blair and J. R. Gardner, *J. Appl. Polym. Sci.*, **27**, 3043 (1982).
- ⁴⁷ N. L. Dias Filho, W. L. Polito and Y. Gushikem, *Talanta*, **42**, 1031 (1995).
- ⁴⁸ M. B. Lohani, A. Singh, D. C. Rupainwar and D. N. Dhar, *J. Hazard. Mater.*, **159**, 626 (2008).
- ⁴⁹ S. W. Al Rmali, A. A. Dahmani, M. M. Abuein and A. A. Gleza, *J. Hazard. Mater.*, **152**, 955 (2008).